Generation of F centres and hole centres in the nonstoichiometric x-ray storage phosphor BaFBr

1998 J. Phys.: Condens. Matter 10 9111

(http://iopscience.iop.org/0953-8984/10/40/014)

J. Phys.: Condens. Matter **10** (1998) 9111–9122. Printed in the UK PII: S0953-8984(98)95485-6

Generation of F centres and hole centres in the nonstoichiometric x-ray storage phosphor BaFBr

S Schweizer†, J-M Spaeth† and T J Bastow†‡

† Universität-GH Paderborn, Warburger Strasse 100A, D-33098 Paderborn, Germany

‡ Materials Characterisation Group CSIRO, Clayton, Victoria 3169, Australia

Received 30 June 1998

Abstract. After x-irradiation of nonstoichiometric $BaF_{1.1}Br_{0.9}$, besides the $F(Br^-)$ centre a new intrinsic hole centre was found by electron paramagnetic resonance (EPR). The powder EPR line of this new centre can be simulated assuming an F_2^- molecule on a fluoride site. The new hole centre is stable at room temperature and is the anti-centre of the $F(Br^-)$ centre in the F centre generation process. Magic angle spinning nuclear magnetic resonance (MAS-NMR) experiments on nonstoichiometric $BaF_{1.1}Br_{0.9}$ show not only resonances of ^{19}F on regular lattice sites, but also resonances which are due to ^{19}F on bromine sites ('fluorine antisites'). There are about 10% fluorine antisites in the nonstoichiometric powder which corresponds to the excess fluorine determined by chemical analysis. The generation of $F(Br^-)$ electron trap–hole trap pairs upon x-irradiation originates at the fluorine antisites.

1. Introduction

BaFBr doped with Eu^{2+} is actually the best x-ray storage phosphor material which is used to generate digital x-ray images. This storage phosphor exhibits a dynamical range of 10^5–10^6 and enhanced sensitivity compared to conventional x-ray films [1].

The physics of information storage in BaFBr involves the generation of electron and hole trap centres proportional to the x-ray dose. In the read-out process the electron trap centres are photostimulated and recombine with the hole trap centres. The recombination energy is transferred to the Eu^{2+} activator which luminesces at 390 nm (e.g. [2]).

For the functioning of the storage phosphors the generation of electron trap and hole trap centres is of prime importance. In BaFBr electrons can be trapped at Br^- vacancies generating $F(Br^-)$ centres and at F^- sites generating $F(F^-)$ centres.

BaFBr powders are normally formed by firing intimate mixtures of BaF_2 and $BaBr_2$. Single crystals are grown by the Bridgman method from a stoichiometric melt of these compounds. It turned out that such BaFBr material is always contaminated with oxygen. The contamination consists of O^{2-} ions on fluoride sites (O_F^{2-}), usually in a concentration of about 10–100 ppm [3]. For charge compensation the O_F^{2-} incorporation leads to the formation of Br^- vacancies in the next or next-nearest position [4], which are necessary for the $F(Br^-)$ centre generation. In the presence of Br^- vacancies x-rays generate $V_K(Br_2^-)$ centres (hole trapped between two adjacent Br^- ions) and $F(Br^-)$ centres, whereby the V_K centres decay at approximately 120 K [5]. Without the presence of Br^- vacancies F centres could only be generated by the so-called F–H process known from alkali halides, in which

0953-8984/98/409111+12$19.50

an exciton decays forming an F–H centre pair (an H centre is a $(\text{halogen})_2^-$ molecular ion on a halide site) [6]. So far, attempts to identify this process in BaFBr have failed in spite of the use of very sensitive methods of optical detection of electron paramagnetic resonance. With electron paramagnetic resonance (EPR) detected via the magnetic circular dichroism of the optical absorption (MCDA-EPR) the F–H pair generation could in principle be investigated. For example, in KBr H centres and F centres were detected with MCDA-EPR and it was found that at 1.5 K the minimal F–H separation for stable F–H pairs is four lattice spacings along a ⟨110⟩ direction [7]. Attempts to identify H centres in stoichiometric oxygen containing BaFBr have so far failed.

The contamination of O_F^{2-} also acts as a competing hole trap centre, since O_F^- centres are formed upon x-irradiation at room temperature [8, 9]. O_F^- centres are, however, not involved in the electron–hole recombination process which leads to the photostimulated Eu^{2+} luminescence (PSL). It must be remarked here that the hole trap centre responsible for the PSL process has not yet been identified [10].

Thus the role of oxygen contamination is both beneficial and detrimental, and it is difficult to control its concentration such as to optimize the performance of these storage phosphors.

An alternative way to produce BaFBr phosphor material is to use NH_4Br instead of $BaBr_2$ as a bromine source. Firing of BaF_2 and NH_4Br leads to nonstoichiometric BaFBr powders with about 10% excess fluorine [11]. This material contains no oxygen contamination. In this nonstoichiometric oxygen-free BaFBr, F centres are generated by x-irradiation at room temperature accompanied by a hole centre as the anti-centre, which is tentatively interpreted as being an H centre in the fluorine sublattice. In this paper EPR and optical spectroscopy are used to investigate this F centre generation mechanism in nonstoichiometric BaFBr powders. Since this nonstoichiometric BaFBr doped with Eu^{2+} is commercially used as x-ray storage phosphor material with excellent figures of merit, in particular for stimulation at lower photon energies, the clarification of the storage mechanism also has important practical implications. In a previous study [12] of the redshift of nonstoichiometric BaFBr doped in addition with Sr^{2+}, it was speculated that the fluorine excess leads to the formation of fluorine antisite defects (F_{Br}^-), which were calculated to be exothermic in BaFBr [13]. Therefore, we also performed magic angle spinning nuclear magnetic resonance (MAS-NMR) experiments in order to check whether this is indeed true. If 10% F_{Br}^- antisite defects were involved in the $F(Br^-)$ centre generation process, than the F centre generation would practically not be 'impurity' limited as in the case of the oxygen contaminated material, and therefore it would be useful for very low up to very high x-ray doses.

2. Experiment

2.1. Sample preparation

BaFBr single crystals were grown in graphite crucibles with the Bridgman method from a stoichiometric mixture of BaF_2 and $BaBr_2$. BaFBr crystallizes in the Matlockite structure [14, 15]. For some of the powder measurements the single crystals were pulverized by means of mortar and pestle.

The stoichiometric BaFBr powder was made by firing intimate mixtures of BaF_2 and $BaBr_2$, whereas the nonstoichiometric BaFBr powder was produced by firing intimate mixtures of BaF_2 and NH_4Br in the ratio of 1:1. The use of NH_4Br as a bromine source results in 10% excess fluorines compared to the stoichiometric BaFBr as was shown

previously by chemical analysis in combination with x-ray diffraction (XRD) methods [11]. Within the measurement accuracy of about 2% a density change of the nonstoichiometric BaFBr powders was not observed [16]. The chemical composition of the BaFBr powders was determined by inductively coupled plasma (Ba) and ion chromatography (F/Br). To test the accuracy of the fluoride determination by ion chromatography, a calibration procedure was performed with 1–5 ppm solutions of NaF. The powders were tested for oxygen contamination by attempting to excite the luminescence due to O_F^{2-} at 500 nm at low temperatures [3]. The stoichiometric BaFBr powder showed O_F^{2-} luminescence, whereas in the nonstoichiometric BaFBr powder no O_F^{2-} luminescence was observed. The weight-based median particle size of the BaFBr powders was 15 μm with a standard deviation of about 10 μm.

When BaF_2 and NH_4Br were mixed and fired in a ratio not deviating from 1:1, a single-phase product was formed. Investigations with x-ray diffraction showed that nonstoichiometric $BaF_{1.1}Br_{0.9}$ has also the Matlockite crystal structure of stoichiometric BaFBr. At most, 1% of other phases could be present [11]. It was not possible to vary the degree of fluorine excess for a single-phase material for which it always turned out to be 10% [16]. For other mixtures the resulting product was multi-phase. Some of the samples were doped with 0.1 mol% Eu^{2+}.

2.2. Spectroscopy

MAS-NMR spectra were recorded with a Bruker MSL 400 spectrometer working at a field of 9.4 T. Operating frequencies of 376.3 MHz for ^{19}F, 108.0 MHz for ^{81}Br, 400.15 MHz for ^{1}H and 44.45 MHz for ^{137}Ba were used. External frequency standards from TMS ($Si[CH_3]_4$) for protons and C_6F_6 for ^{19}F, NaCl (aq) for ^{23}Na, NH_4Br for ^{81}Br and $BaZrO_3$ for ^{137}Ba were taken. Magic angle spinning was done with a 4 mm rotor in a Bruker probe with a double-bearing gas turbine at a rotation frequency of 12 and 14 kHz. The ^{81}Br spectra were recorded using a solid echo pulse sequence, ^{19}F and ^{1}H spectra using single-pulse acquisition. The ^{19}F spectra were recorded using a 20 s pulse sequence repetition time. In order to check whether the repetition time was longer than the relevant relaxation times for ^{19}F lattice nuclei and ^{19}F antisites, an additional ^{19}F spectrum was run at 100 s repetition time, which confirmed that the relative intensities of the lines of F lattice nuclei and antisites remained the same.

EPR measurements were performed with a computer-controlled custom-built EPR spectrometer. The usual measurement temperature was about 10–15 K. The powder samples were filled in quartz glass sample holders and x-irradiated at room temperature (tungsten anode, 50 kV, 30 mA, 120 min) and at temperatures below 77 K (tungsten anode, 60 kV, 15 mA, 120 min), respectively. Because of the irradiation defects in the quartz glass sample holder the powders were filled in another quartz glass sample holder after the x-irradiation. Unfortunately, this was only possible after x-irradiation at room temperature.

Luminescence and luminescence excitation spectra (in particular, PSL excitation spectra) were measured with a single-beam spectrometer in which 0.25 m double monochromators (Spex) were available for excitation and luminescence. After x-irradiation at room temperature (tungsten anode, 60 kV, 15 mA, 60 s) the samples were excited with a halogen lamp. UV-visible luminescence was detected using single-photon counting with a photomultiplier.

3. Experimental results

3.1. Photostimulated luminescence measurements

Figure 1 shows the PSL excitation spectra of (a) stoichiometric BaFBr:Eu powder and (b) nonstoichiometric $BaF_{1.1}Br_{0.9}$:Eu powder. The PSL peak of the stoichiometric sample is at 540 nm while that of the nonstoichiometric one is at 580 nm, i.e. at lower photon energy, and there is an additional shoulder at 510 nm. The intensity ratio between the 580 nm peak and the high-energy shoulder at 510 nm is approximately 2:1. In both materials the luminescence is due to the stimulation of $F(Br^-)$ and $F(F^-)$ centres. The absorption peak of $F(Br^-)$ centres is at 580 nm for the electrical light vector perpendicular to the crystal c-axis, while it is at 510 nm for $\boldsymbol{E}\|\boldsymbol{c}$. For $F(F^-)$ centres the absorption peaks are at 470 nm for $\boldsymbol{E}\perp\boldsymbol{c}$ and at 520 nm for $\boldsymbol{E}\|\boldsymbol{c}$ [17]. It is seen qualitatively in figure 1 that fluorine excess (figure 1, curve (b)) leads to an enhanced concentration of $F(Br^-)$ centres [12]. The absorption peaks of $F(Br^-)$ centres agree well with the peak and shoulder of figure 1, curve (b). The intensity ratio of 2:1 is caused by the statistical distribution of the parallel and perpendicular crystallite orientations with respect to the electrical light vector. Apparently in the nonstoichiometric BaFBr very few $F(F^-)$ centres are generated in comparison to $F(Br^-)$ centres.

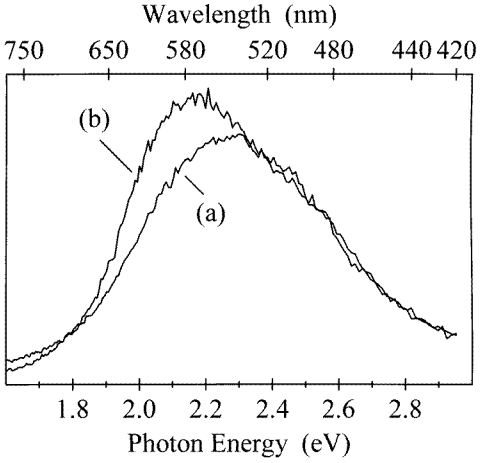

Figure 1. PSL excitation spectra measured at room temperature of (a) stoichiometric BaFBr:Eu powder and (b) nonstoichiometric $BaF_{1.1}Br_{0.9}$:Eu powder after x-irradiation at room temperature.

3.2. EPR measurements

After x-irradiation at room temperature we found in stoichiometric BaFBr powder an EPR line that is due to the O_F^- centre (figure 2, spectrum (a)). Note that we could excite an O_F^{2-} luminescence at 500 nm in this stoichiometric BaFBr powder. The EPR line in the field range between 335 and 350 mT is caused by the $F(Br^-)$ centre. The EPR spectrum of the O_F^- centre was identified previously in O_F^{2-} containing single crystals after x-irradiation at room temperature [8, 9]. We compared the EPR spectrum (a) of figure 2 to that measured in a pulverized oxygen containing single crystal, the EPR of which contained only O_F^- and the $F(Br^-)$ centres at 10 K before pulverizing. Both powder spectra were identical.

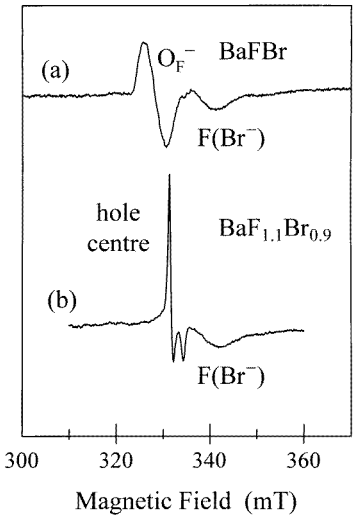

Figure 2. Powder EPR spectra of (a) stoichiometric and (b) nonstoichiometric BaFBr powder after x-irradiation at room temperature, measured at 10 K applying a microwave frequency of 9.335 GHz.

In nonstoichiometric BaFBr powders we could not excite an O_F^{2-} luminescence. This powder is obviously oxygen-free. The EPR spectrum of nonstoichiometric BaFBr powder (figure 2, spectrum (b)) shows, after x-irradiation at room temperature, besides the EPR line of the F(Br^-) centre a powder EPR line whose g values indicate that it is probably caused by a new hole centre, since it can be simulated well by assuming an axial centre with the g values of $g_\perp = 2.02$ and $g_\parallel = 2.002$. The positive g-shift indicates that we deal here with a hole centre, one which has not yet been reported before in BaFBr. Its nature as a hole centre is further supported by the observation that its intensity increases proportional to the x-ray dose as does that of the F(Br^-) centre. When bleaching with light into the F(Br^-) absorption band at room temperature, both F(Br^-) and the new hole centre are destroyed simultaneously. After loosing all F centres, only about 30% of the hole centre are left. The observation strongly suggests that the F(Br^-) centre and the new hole centre are generated as a pair of electron and hole trap centres as a result of electron and hole separation by the x-rays. Stimulation of the F(Br^-) centres recombines the electrons with the holes of the new hole centre.

After x-irradiation of stoichiometric BaFBr powder at temperatures below 77 K we observed intense resonance lines of the $V_K(Br_2^-)$ centres and a weak EPR signal of the F(Br^-) centres. After annealing up to 300 K, the $V_K(Br_2^-)$ centre lines have disappeared whereas the O_F^- centre line appears. The $V_K(Br_2^-)$ centre decays at about 120 K [5]. The moving hole is trapped by an O_F^{2-} impurity to form the O_F^- centre [4].

After x-irradiation at temperatures below 77 K the EPR spectrum of the non-stoichiometric BaFBr powder showed again intense resonance lines of the $V_K(Br_2^-)$ centres and a weak signal of the F(Br^-) centres, as well as the powder EPR line of the new hole centre described above. When using a low x-ray dose a rather strong signal of the V_K centres appears relative to that of the new hole centres. Upon increasing the x-ray dose, the signal of the new hole centre gains rapidly while that of the V_K centres grows at a slower

rate. The experiments were not carried as far as reaching a saturation of the V_K centre signal, but it appears that such a saturation can be reached while no sign of an incipient saturation was observed for the new hole centre.

After annealing up to 300 K the $V_K(Br_2^-)$ centre EPR lines have disappeared. This thermal decay of the $V_K(Br_2^-)$ centre did not cause a change in the EPR line intensity of the new hole centre, but part of the F centre signal was destroyed. Unfortunately, the signal-to-noise ratio of the F centre was not good enough, in order to check whether as many F centres were destroyed as V_K centres have disappeared.

3.3. Nuclear magnetic resonance measurements

Figure 3 shows the MAS spectra of ^{19}F of a pulverized stoichiometric single crystal of BaFBr (spectrum (a)) and of the nonstoichiometric $BaF_{1.1}Br_{0.9}$ powder (spectrum (b)). The peaks due to the lattice ^{19}F nuclei of both spectra coincide within experimental error at 150.9 ppm. At lower frequency, at 145.3 ppm, a new line appears in the nonstoichiometric $BaF_{1.1}Br_{0.9}$ which also shows up in the spinning side bands. The intensity of the new line as measured by the area in comparison to that of the lattice ^{19}F nuclei is 7.3%. Extending the analysis to the contributions of the spinning side bands yields altogether 8.6%. Thus, the new line at almost 6 ppm to lower frequency is due to approximately 9% of ^{19}F nuclei with a different site compared to the lattice nuclei. This is close to the 10% excess of F in the lattice determined by chemical analysis [11]. Since for electrostatic reasons it is very unlikely that the new site is an interstitial site, we assign the new line to F^- on Br^- vacant sites, i.e. to F^- antisites.

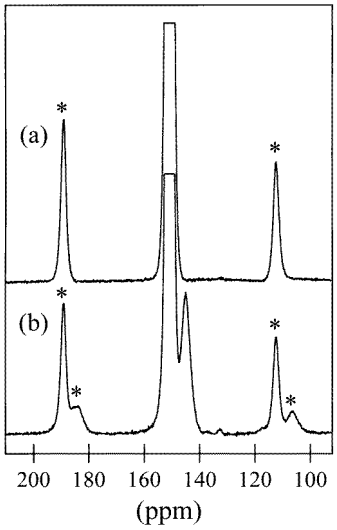

Figure 3. ^{19}F MAS spectra of (a) a crushed stoichiometric BaFBr single crystal and (b) nonstoichiometric $BaF_{1.1}Br_{0.9}$ powder. The spinning side bands are marked with asterisks.

Figure 4 shows the high- and low-frequency edge singularities of the ^{137}Ba static powder spectrum having second-order quadrupole interaction [18]. The ^{137}Ba lineshapes are a superposition of two spectra taken with two different frequency offsets, each near a respective edge. Because of the 4 μs pulses in the echo sequence, only a 250 kHz

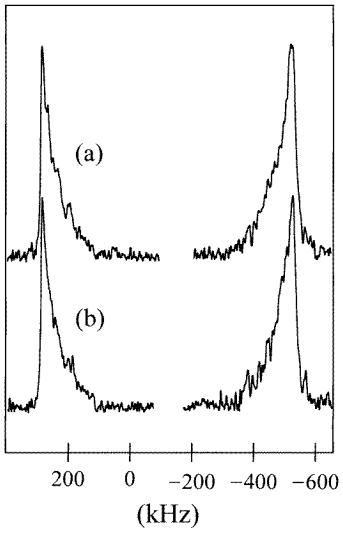

Figure 4. Edge singularities for ^{137}Ba of (a) a crushed stoichiometric BaFBr single crystal and (b) nonstoichiometric $BaF_{1.1}Br_{0.9}$ powder.

wide section of the total ^{137}Ba spectrum was observed at each offset frequency. Although the central portion of the spectrum could be observed in the same manner, it was only necessary to observe the two edges to establish the equality of $C_Q = e^2qQ$ (of ^{137}Ba) in both BaFBr samples. The edge singularities are identical for both the stoichiometric and nonstoichiometric BaFBr also showing that the F^- excess does not change the crystal structure. The lattice parameters, i.e. the near geometry, must be almost identical for both crystals, since the positions of the edge singularities of the Br and Ba second-order quadrupole perturbed powder patterns are identical within experimental error. Note, that the electrical field gradients vary as r^{-3}. However, there are also in the nuclear magnetic resonance (NMR) spectra indications that the nonstoichiometric material contains a small fraction of another phase. In figure 5 the static powder spectra of ^{81}Br for both materials are compared. The $1/2 \rightarrow -1/2$ NMR transitions show different second-order quadrupole interaction perturbed line shapes: the nonstoichiometric material has an extra line in the centre, which is a narrow line not influenced by quadrupole interactions and thus must come from Br sites which experience no electrical field gradient. A rough estimate of the intensity of the line compared to the other ^{81}Br lattice nuclei yields a value of approximately 1%. Since the material was made by a reaction of BaF_2 and NH_4Br, a natural assumption would be to assume that some NH_4Br has been incorporated. NH_4Br has a cubic structure and therefore vanishing quadrupole interactions and in addition the ^{81}Br shift in NH_4Br is the same as that found here. However, we found neither the expected ^{14}N nor the ^{1}H signals for NH_4Br. In particular, the latter should have been seen in NH_4Br had it been present. Thus, we must leave as an open question which subphase causes the 'cubic' ^{81}Br signals.

It is interesting to compare the MAS spectra of ^{19}F in BaF_2 (at 152.7 ppm) to those of BaFBr and/or $BaF_{1.1}Br_{0.9}$. Apart from a slight difference in chemical shift, there is a pronounced difference in line width: the half width is 4.2 ppm in BaF_2 and it is 1.65 ppm in both BaFBr samples. In BaF_2 the dipole–dipole interaction between the ^{19}F lattice nuclei is higher compared to BaFBr where this interaction is 'diluted' by the presence of Br.

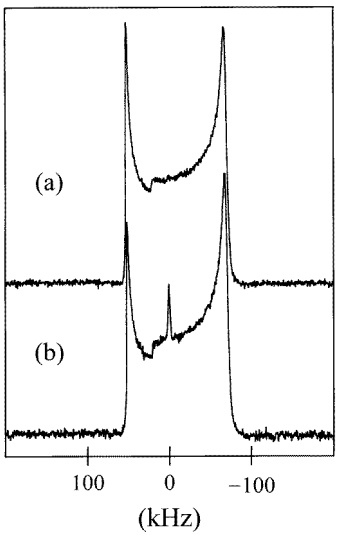

Figure 5. The ^{81}Br $1/2 \rightarrow -1/2$ NMR transition with second-order quadrupole perturbed line shape of (a) a crushed stoichiometric BaFBr single crystal and (b) nonstoichiometric $BaF_{1.1}Br_{0.9}$ powder.

4. Discussion

The generation of $F(Br^-)$ centres in stoichiometric, oxygen containing BaFBr is facilitated by the presence of Br^- vacancies as charge compensators for the O_F^{2-} centres. At temperatures below 200 K only $F(Br^-)$ centres are generated upon x-irradiation [4]. $F(F^-)$ centres are observed only after x-irradiation above 200 K. The mechanism for their formation has not yet been clarified [4, 17]. It seems that a thermally activated process is necessary. However, their production does not proceed at the expense of the generated $F(Br^-)$ centres as primary F centres [4]. No F–H process was ever observed in this material. Had it occurred, as it does in the alkali halides, we would have been able to observe it with MCDA and MCDA-EPR.

The generation of F centres in nonstoichiometric $BaF_{1.1}Br_{0.9}$ powders seems to occur via two mechanisms. At 77 K two kinds of hole centres were observed: $V_K(Br_2^-)$ centres and the new hole centres, which we believe are H centres in the F^- sublattice (see later). The $V_K(Br_2^-)$ centre generation at 77 K seems to indicate that in spite of no oxygen contamination the nonstoichiometric BaFBr also contains Br^- vacancies. Upon annealing to room temperature the $V_K(Br_2^-)$ centres and part of the $F(Br^-)$ centres disappear: mobile $V_K(Br_2^-)$ centres recombine with $F(Br^-)$ centres. However, $F(Br^-)$ centres remain and so does the EPR signal of the new hole centre, which is not changed at all upon the availability of mobile $V_K(Br_2^-)$ centres.

The question arises of what is the mechanism of creation of the new hole centre and $F(Br^-)$ centres. As shown in our experiments, the new hole centre is an anti-centre of the $F(Br^-)$ centre, i.e. both are simultaneously generated and both disappear upon bleaching into the $F(Br^-)$ centre absorption band. The fact that upon bleaching of the $F(Br^-)$ centre absorption band about 30% of the new hole centres survive can be explained by the argument that some $F(Br^-)$ centres form F aggregate centres upon bleaching, i.e. not all of them recombine with their anti-centres, i.e. the new hole centre. The nonstoichiometric $BaF_{1.1}Br_{0.9}$ powder differs from the stoichiometric one in that there

is no oxygen contamination and that 10% of the Br^- anions are replaced by F^-, i.e. there are 10% F^- antisite defects. This was shown by the MAS-NMR experiments. There is a new ^{19}F species with a chemical shift different from that of the ^{19}F of the host crystal and a relative intensity tying in well with the F^- excess determined chemically [11]. Since this NMR signal is very unlikely to originate from F^- interstitials for electrostatic reasons, we assign the new MAS lines to F^- antisites. The MAS spectra confirm an earlier suggestion that the F^- to Br^- ratio of about 1.1 to 0.9 is achieved by 10% enhanced fluorine incorporation and a simultaneous 10% bromine reduction [12]. In this case a charge compensation on the cationic sublattice is not necessary, so that there is no density change within experimental error of $\pm 2\%$ [16]. The MAS-NMR spectra of Ba^{2+} and Br^- show that apart from the antisites the normal Matlockite structure is realized in this nonstoichiometric material in agreement with previous XRD studies [11].

The two chemical shifts found for ^{19}F for the regular F lattice site and the antisite ^{19}F are not very different from each other: 150.9 ppm for the regular sites, 145.3 ppm for the antisites. The difference of 5.6 ppm is smaller than that found for ^{19}F in the divalent fluorides CaF_2, SrF_2 and BaF_2 (see, e.g., [19, 20]) which vary between 58 ppm and 152 ppm. It is interesting to note that the Ba^{++}–F^- distance in BaF_2 (2.68 Å) is almost identical to that in BaFBr (2.66 Å). Boden *et al* [19] argued that the chemical shift is determined by the metal–F^- distance. The 150.9 ppm found for the regular ^{19}F lattice nuclei tie in well with this rule. Not so the ^{19}F antisites (F^- at Br^- site), which have a distance of 3.36 Å to the next Ba neighbour (along the *c*-axis) and 3.42 Å to the four next-nearest Ba neighbours. Perhaps the larger screening is the result of a larger site for F^- and the more expanded electron core.

Since $F(Br^-)$ centres and the new hole centre are electron and hole trap centres created simultaneously and proportional to each other, it is suggested that F^- antisites (F^-_{Br}) are the origin of the $F(Br^-)$ centres and the new hole centre according to the reaction

$$F^-_{Br} \xrightarrow{\text{x-ray}} F(Br^-) + F^-_{2,F}$$

i.e. an $F(Br^-)$ and an F_2^- molecular centre in the F^- sublattice ($F^-_{2,F}$) are created in an F–H process where the electron trap centre (F centre) is formed in the Br^- sublattice and the H centre is formed in the F^- sublattice. To support this suggestion, we analyse in more detail the powder EPR spectra of the new H centre. It is known that F_2^- molecular centres on F^- sites can be produced in alkali-earth fluorides by x-irradiation below 77 K [21]. There, the two fluorine nuclei of the H-type centre are not equivalent, i.e. one fluorine nucleus is placed on an interstitial site ('fluorine interstitial') whereas the second one is on a regular lattice site ('fluorine substitutional'). The hyperfine (hf) interactions of the fluorine interstitial and the fluorine substitutional are different. Figure 6, spectrum (a), shows a calculated powder EPR spectrum of a F_2^- centre with two inequivalent fluorine nuclei. The *g* tensor and the two hf interaction tensors are axial. We hereby roughly assumed the fluorine hf interaction values of H-type F_2^- centres in alkaline-earth fluorides [21], i.e. $A_\perp(1) = 200$ MHz and $A_\parallel(1) = 2000$ MHz for the first nucleus and $A_\perp(2) = 500$ MHz and $A_\parallel(2) = 3000$ MHz for the second one, respectively. A comparison with figure 2, spectrum (b), shows that it is not possible to simulate the powder EPR line of the new hole centre by assuming a F_2^- centre with two inequivalent fluorine nuclei.

Figure 6, spectrum (b) and spectrum (c), shows two calculated powder EPR spectra of an F_2^- centre with two equivalent fluorine nuclei. We hereby assumed typical fluorine hf interaction values [21] of $A_\perp = 200$ MHz and $A_\parallel = 2000$ MHz or $A_\perp = 20$ MHz and $A_\parallel = 2000$ MHz, respectively. In both cases the powder EPR lines indicating the hf interaction for an orientation parallel to the molecular axis are very weak. In figure 6,

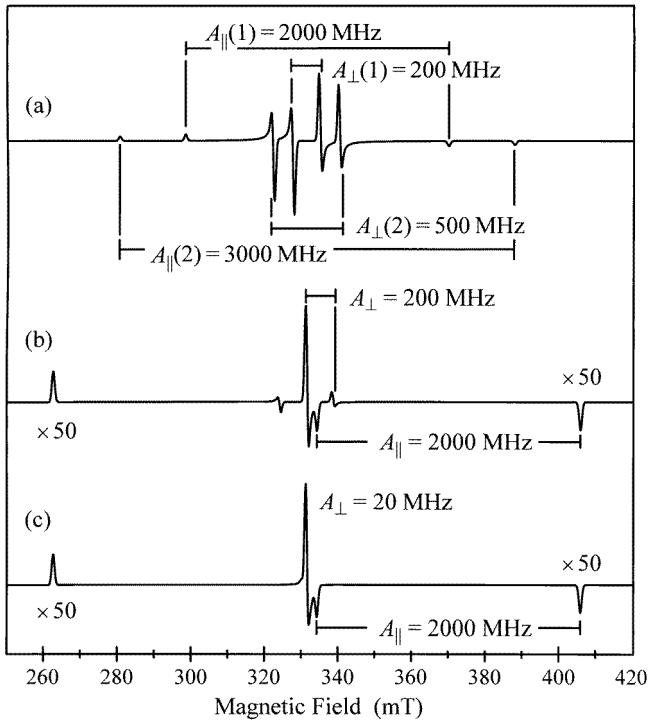

Figure 6. Calculated powder EPR spectra of a F_2^- centre with (a) two inequivalent fluorine nuclei, (b) and (c) two equivalent fluorine nuclei. The g tensors with $g_{\perp} = 2.02$ and $g_{\|} = 2.002$ are axial as well as the ^{19}F hyperfine tensors. The bars indicate the corresponding hyperfine splittings. The microwave frequency is 9.335 GHz.

spectrum (b) and spectrum (c), the lines are scaled up by a factor of 50. The powder EPR lines indicating the hf interaction perpendicular to the molecular axis are clearly visible in figure 6, spectrum (b). If we assume a small value for $A_{\perp}$ ($= 20$ MHz), the hf lines are superimposed by the central lines (figure 6, spectrum (c)). Thus, by comparison with figure 2, spectrum (b), we assume the hole centre to have $A_{\perp} \leqslant 20$ MHz.

Figure 7 shows the F_2^- centre in BaFBr with two equivalent fluorine nuclei. The molecular axis of the F_2^- centre with the two equivalent fluorine nuclei is parallel to the *a*-axis (*b*-axis) of the crystal as calculated in [22]. Since a powder EPR spectrum is a summation over all possible orientations of the magnetic field vector (e.g. [23]), the information about the orientation of the interaction tensors to the crystal axes is lost. Therefore, the measured powder EPR spectrum of the new hole centre does not allow us to decide on the position of the molecular axis.

A qualitative view of the F–H process would be that the valence electron of the F^- antisite is excited upon an exciton decay at the antisite into a diffuse excited state and that the F^0 becomes mobile and moves to the F^- sublattice, where it associates itself with a lattice F^- to form the $H(F_2^-)$ centre on a fluoride site. It was calculated by Baetzold [22] that such an H centre is stable and also that the formation of F_{Br}^- antisites is exothermic in BaFBr [13]. We cannot say though whether the $F(Br^-)$ and H centres are nearest neighbours or further apart. Judging from the results obtained in the alkali halides, they will be further apart, otherwise they would probably recombine [7].

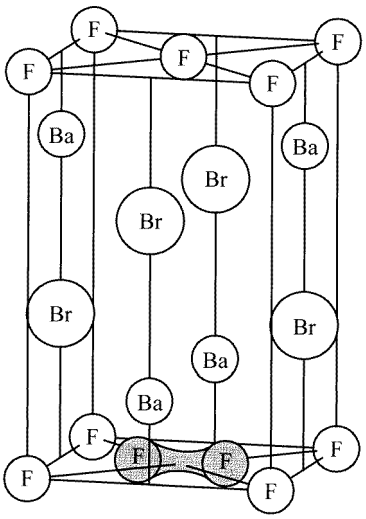

Figure 7. Model of an H-type F_2^- centre in BaFBr with two equivalent fluorine nuclei after [22].

To be stable at room temperature it is important for the hole centre to escape recombination with the F centre. It seems reasonable to argue that the hole can move away more easily from the F centre in the F sublattice than in the Br sublattice. This is because the F^-–F^- distance is much shorter (3.18 Å) than the Br^-–Br^- distance, whether in the plane (4.50 Å) or out of the plane (3.72 Å). Also there is a linear (110) or (100) chain of equivalent F^- ions, whereas the hole motion within the Br^- double layer would need to proceed in a zigzag motion to separate from the F centre. The former pathway resembles more the situation in the alkali halides, where the hole motion is known to proceed along the (110) halogen chain.

The experimental observation that the V_K centre production seems to saturate upon increasing the x-ray dose, while that of the H centre production showed no sign of it, is in line with our interpretation. The maximum number of V_K centres depends on the number of Br^- vacancies present, which cannot be excessively large, as otherwise a significant change of the density would have been observed. Although, because of the powder spectra, we cannot easily determine the number of V_K centres quantitatively, it will be of the order of 10^{16}–10^{17} cm^{-3} and that should be the order of magnitude of the Br^- vacancies present. On the other hand, F^- antisite defects are 'abundant' (10%) in comparison. So, no saturation in H centre production is expected in line with our proposed model. The decay of the $V_K(Br_2^-)$ centres did not influence the EPR line intensity of the new hole centre (see previously). Had the moving holes of the decaying $V_K(Br_2^-)$ centres been trapped by F^- interstitials, the EPR signal of $H(F_2^-)$ hole centres would have been enhanced. This was not the case. Therefore, we suggest that the $F(Br^-)$ centre production in nonstoichiometric BaFBr and the simultaneous generation of the hole F_2^- centre is caused by F^- antisites and not by F^- interstitials.

Unfortunately, we cannot investigate by EPR nonstoichiometric $BaF_{1.1}Br_{0.9}$ doped with Eu^{2+} in order to find out whether at room temperature the $F(Br^-)$–H centres are the responsible electron–hole trap centres for the PSL effect or whether at 77 K V_K centres play the sole role of the hole centres or whether both centres are active. The reason is that the EPR spectrum of Eu^{2+} centres, doped at the 1000 ppm level, are very strong and

superimposed on the EPR lines of the V_K and H centres. The fact that upon warming to room temperature the V_K centres and thus a substantial fraction of the $F(Br^-)$ centres decay, together with the fact that F bleaching destroys the new H centre, makes the new H centre indeed very likely to be responsible for the PSL process. More experiments, however, such as the careful study of the PSL effect as a function of the x-ray dose in comparison with the V_K and F centre formation as a function of the dose, are needed to establish this. Such experiments are planned for the future.

In summary, we have shown that in nonstoichiometric $BaF_{1.1}Br_{0.9}$ there are 10% F^- antisite defects, which, upon x-irradiation, are decomposed in $F(Br^-)$ and $H(F_2^-)$ centres as electron and hole trap centres, which are created and bleached simultaneously. This is the first F–H process established in BaFBr. No F–H process seems to exist within one sublattice: no $F(Br^-)$–$Br_{2,Br}^-$ or $F(F^-)$–$F_{2,F}^-$ centre pairs have been observed so far. The F–$H(F_{2,F}^-)$ process discovered here is promising for the use of $BaF_{1.1}Br_{0.9}$ x-ray storage phosphors for very high x-ray doses, since the creation of F centres does not seem to be impurity limited as it is in stoichiometric, oxygen-containing BaFBr.

Acknowledgments

The authors would like to thank Dr P Willems and Dr P J R Leblans of the Agfa-Gevaert company (Mortsel, Belgium) for continuous support and many helpful discussions.

References

[1] Sonoda M, Takano M, Miyahara J and Kato H 1983 *Radiology* **148** 833
[2] Blasse G 1993 *J. Alloys Comp.* **192** 17
[3] Koschnick F-K, Hangleiter Th, Song K S and Spaeth J-M 1995 *J. Phys.: Condens. Matter* **7** 6925
[4] Koschnick F-K, Spaeth J-M and Eachus R S 1992 *J. Phys.: Condens. Matter* **4** 3015
[5] Hangleiter Th, Koschnick F-K, Spaeth J-M, Nuttall R H D and Eachus R S 1990 *J. Phys.: Condens. Matter* **2** 6837
[6] Fowler W B 1968 *Physics of Color Centers* (New York: Academic)
[7] Meise W, Rogulis U, Koschnick F-K, Song K S and Spaeth J-M 1994 *J. Phys.: Condens. Matter* **6** 1815
[8] Eachus R S, McDugle W G, Nutall R H D, Olm M T, Koschnick F-K, Hangleiter Th and Spaeth J-M 1995 *J. Phys.: Condens. Matter* **3** 9327
[9] Eachus R S, McDugle W G, Nutall R H D, Olm M T, Koschnick F-K, Hangleiter Th and Spaeth J-M 1995 *J. Phys.: Condens. Matter* **3** 9339
[10] Spaeth J-M, Hangleiter Th, Koschnick F-K and Pawlik Th 1995 *Radiat. Effects Defects Solids* **135** 1
[11] Klee R J 1995 *J. Phys. D: Appl. Phys.* **28** 2529
[12] Dietze C, Hangleiter Th, Willems P, Leblans P J R, Struye L and Spaeth J-M 1996 *J. Appl. Phys.* **80** 1074
[13] Baetzold R C 1987 *Phys. Rev.* B **36** 9182
[14] Liebich B W and Nicollin D 1977 *Acta Crystallogr.* B **33** 2790
[15] Beck H P 1979 *Z. Anorg. Allg. Chem.* **451** 73
[16] Willems P 1996 Private communication (Agfa-Gevaert, Mortsel, Belgium)
[17] Koschnick F-K, Hangleiter Th, Spaeth J-M and Eachus R S 1992 *J. Phys.: Condens. Matter* **4** 3001
[18] Cohen M H and Reif F 1957 *Solid State Phys.* **5** 321
[19] Boden N, Kahal P K, Mee A, Mortimer M and Peterson G N 1983 *J. Magn. Reson.* **54** 419
[20] Vaughan R W, Elleman D D, Rhim W-K and Stacey L M 1972 *J. Chem. Phys.* **57** 5383
[21] Hayes W 1974 *Crystals with the Fluorite Structure* (Oxford: Clarendon)
[22] Baetzold R C 1989 *J. Chem. Phys. Solids* **50** 915
[23] Wertz J E and Bolton J R 1972 *Electron Spin Resonance* (New York: McGraw-Hill)